Pediatric Radiology (2022) 52:1786–1798
https://doi.org/10.1007/s00247-022-05376-w

PICTORIAL ESSAY

Spectrum of bowel wall thickening on ultrasound with pathological correlation in children

Ione Limantoro[1] · Anna F. Lee[2] · Daniel G. Rosenbaum[1]

Received: 22 October 2021 / Revised: 4 March 2022 / Accepted: 1 April 2022 / Published online: 6 May 2022

Abstract
Applications for bowel US in children have been well described; however, less focus has been placed on patterns of bowel wall architectural change in specific disease states. This pictorial essay reviews normal bowel wall architecture and covers a variety of inflammatory, infectious, vascular and neoplastic disorders outside the neonatal period as seen on US, with illustrative pathological correlation. A thorough understanding of normal and abnormal bowel wall architecture can enrich sonographic interpretation and provide a valuable adjunct to appropriate clinical investigation.

Keywords Bowel wall · Children · Colon · Gastrointestinal tract · Inflammatory bowel disease · Radiology–pathology correlation · Small bowel · Thickening · Ultrasound

Introduction

Ultrasound has long been the mainstay in diagnosing select pediatric gastrointestinal disorders such as pyloric stenosis, intussusception and appendicitis, and has been incorporated into many standard imaging schemes for diagnosing and monitoring inflammatory bowel disease (IBD) [1, 2]. The modality's versatility in assessing positional, intraluminal and extramural abnormalities has been well documented; however, one of its strengths lies in the delineation of mural architecture afforded by its spatial resolution [3, 4]. In clinical practice we periodically encounter comments alluding to nonspecific bowel wall thickening, which adds limited value to patient care. Although there is overlap in sonographic findings among categories of disease, and pathognomonic features are uncommon, a thorough understanding of normal and abnormal bowel wall architecture can inform differential considerations and complement clinical evaluation.

✉ Daniel G. Rosenbaum
Daniel.Rosenbaum@cw.bc.ca

[1] Department of Radiology, British Columbia Children's Hospital, University of British Columbia, 4500 Oak St., Vancouver, BC V6H 3N1, Canada

[2] Department of Pathology and Laboratory Medicine, British Columbia Children's Hospital, University of British Columbia, Vancouver, BC, Canada

Technique for pediatric bowel ultrasound

Application and technique for bowel US are contextual and subject to the practicalities of the clinical scenario. Targeted studies performed portably can be expedient in critically ill children even if US is not the first-line imaging test, i.e. in the identification of management-altering findings such as bowel ischemia, torsional phenomena or suspected perforation. In these emergent situations no preparation is required, whereas in the non-urgent setting keeping children nil per os (NPO) for 4 h helps minimize bowel gas. Initially, a lower-frequency curvilinear transducer (i.e. 1–6 MHz or 2–9 MHz, depending on patient size) can be used to screen the abdomen for orientation to anatomy and detection of global changes. Dedicated assessment of the bowel using higher-frequency linear-array transducers (12–20 MHz) and graded compression is then performed for detailed evaluation of the bowel wall, generally starting at the terminal ileum and moving antegrade along the colon, with potential adjustments including intercostal imaging for evaluation of the splenic flexure and a return to a lower-frequency transducer for visualization of the distal rectosigmoid colon [5]. Assessment should include evaluation of bowel wall architecture, thickness and vascularity in both transverse and sagittal planes. The remainder of the small bowel is evaluated in an overlapping "lawnmower" manner, moving vertically across the abdomen in the transverse plane, beginning in the right lower quadrant and ending in the left lower quadrant

[6]. Additional findings such as bowel motility, mesenteric changes, lymphadenopathy and fluid collections are documented throughout the examination.

Normal bowel wall architecture

Histologically, the gastrointestinal tract is divided into four layers: the innermost mucosa (encompassing the epithelium, lamina propria and muscularis mucosae), the submucosa, the muscularis propria (composed of two layers of smooth muscle in the small and large bowel and three layers in the stomach) and the outermost serosa. Each layer plays a variable role in digestion and absorption, secretion, immunoresponse and motility, and the layers might be differentially affected in particular disease states [7]. The lamina propria within the mucosa, for example, contains abundant lymphoid tissue, and lymphatics and might appear prominent in immunologically active regions such as the Peyer patches within the terminal ileum, as well as in diseases inciting vigorous immune response. The submucosa, in addition to containing inflammatory cells, autonomic nerve fibers and lymphatics, contains a complex distribution network for arteries and small venous channels and therefore commonly thickens in states of hypervascularity or venous congestion. Because US relies on reflection and attenuation at tissue interfaces, the bowel wall appears sonographically as five layers of alternating echogenicity, the so-called gut signature. This stratified pattern consists of an inner echogenic mucosal interface, hypoechoic mucosa, echogenic submucosa, hypoechoic muscularis propria and echogenic serosa (Fig. 1), although not all layers are visible in all cases, depending on luminal content, mesenteric characteristics and spatial resolution. In most benign conditions the gut signature is preserved,

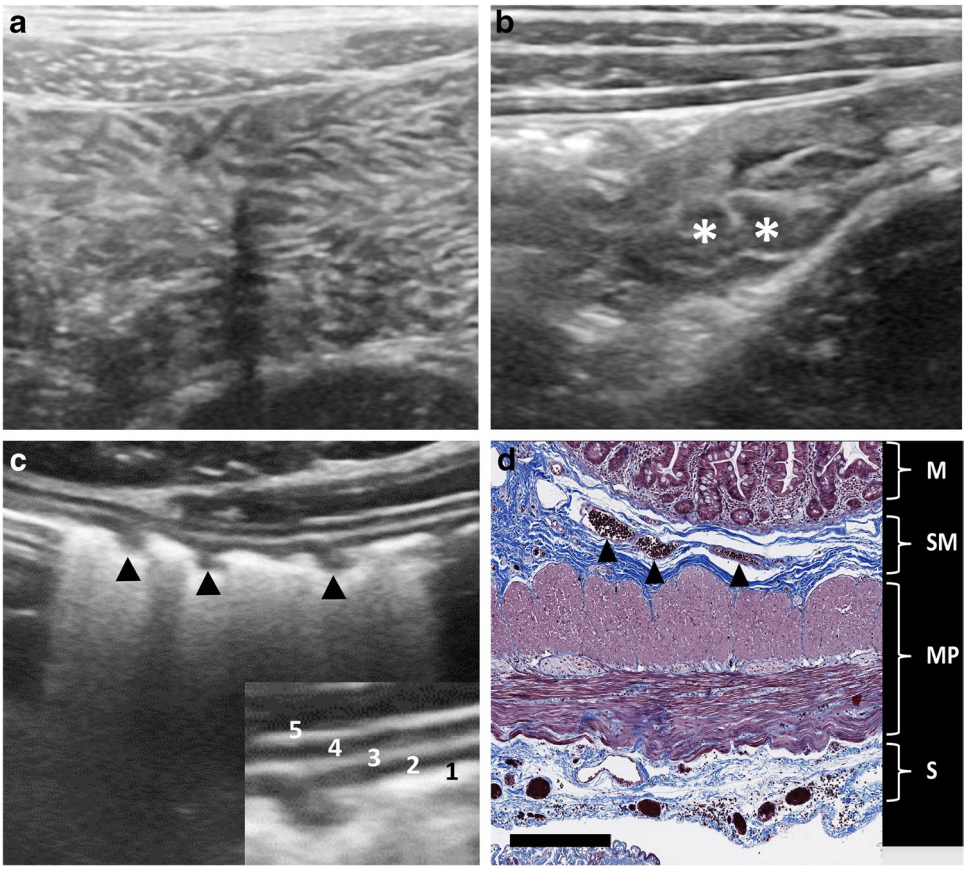

Fig. 1 Normal mural architecture of select bowel segments in a 14-year-old boy. **a** Transverse gray-scale US image of the normal jejunum shows a feathery appearance of the bowel because of tightly packed valvulae conniventes, which are more sparsely distributed in the ileum. **b** Transverse gray-scale US of the normal terminal ileum demonstrates a prominent hypoechoic mucosa with a nodular or pebbly appearance (*asterisks*) caused by hyperplastic lymphoid follicles. **c** Transverse gray-scale US of the normal transverse colon shows evenly spaced pyramidal haustra (*arrowheads*). Inset illustrates the multilaminar structure of bowel wall encompassing the echogenic mucosal interface (*1*), hypoechoic mucosa (*2*), echogenic submucosa (*3*), hypoechoic muscularis propria (*4*) and outer serosal interface (*5*). **d** Trichrome stain of normal small bowel (bar=300 μm). The four histological layers of bowel are visible, encompassing mucosa (*M*), submucosa (*SM*), inner circular and outer longitudinal layers of the muscularis propria (*MP*), and serosa (*S*). Blood vessels traverse the submucosa (*arrowheads*), accounting for disproportionate thickening of this layer in many inflammatory conditions

whereas in more severe inflammatory or neoplastic disorders the layered wall architecture can be focally disrupted or lost entirely (Fig. 2) [3, 8, 9]. Reported ranges for normal bowel wall thickness in children vary in the literature and increase slightly with age; however, an approximate wall thickness of 2.5 mm in the small bowel and 2.0 mm in the colon is usually appropriate [3, 10, 11].

An understanding of normal bowel wall architecture can help refine diagnosis and avoid pitfalls. Documentation of a gut signature, for instance, is considered a confirmatory finding for gastrointestinal duplication cysts, which contain all of the normal bowel layers and share a common muscularis propria with their parent bowel segments. Visualization of bowel wall architecture or its absence can also help correctly identify potential mimics of bowel pathology such as infiltrative or diffuse peritoneal diseases. Plexiform neurofibromas of the mesentery are an uncommon manifestation of neurofibromatosis type 1 that arise along the autonomic nerves accompanying mesenteric vessels or along serosal nerves. Lesions can assume a tubular or multilobular appearance, vaguely resembling collapsed bowel loops, but should be differentiated based upon a targetoid rather than stratified sonographic appearance, with central echogenic collagenous and peripheral hypoechoic myxoid components [12–14]. Peritoneal dissemination of tumor is likewise uncommon in children but can be seen with Burkitt lymphoma, malignant ovarian neoplasms and rhabdomyosarcoma, among others. Peritoneal rhabdomyosarcoma in particular has been observed to produce a cerebriform pattern on US resembling matted or thickened bowel loops but lacking a true gut signature (Fig. 3) [14, 15].

Infection and inflammation

Crohn disease

The role of US in IBD varies worldwide. In Europe, US has historically played a greater role in IBD management and is cited alongside MR enterography as a preferred modality for diagnosing and monitoring disease in the joint consensus guidelines of the European Crohn's Colitis Organisation (ECCO) and the European Society of Gastrointestinal and Abdominal Radiology (ESGAR) [16]. In North America, US has assumed a more limited role as a complementary modality or problem-solving tool, although more widespread application of contrast-enhanced ultrasound (CEUS) and US elastography is likely to continue to augment its contribution [17, 18]. US can be of particular benefit in assessing terminal ileal Crohn disease because of its reliable identification of this segment and its usefulness in children who are too young to undergo MR enterography without sedation and in children who require frequent imaging follow-up [19].

The hallmark of active Crohn disease on US is bowel wall thickening and hypervascularity predominantly affecting the submucosa. Asymmetrical mural thickening along the mesenteric side of bowel has been cited as a fairly specific feature of Crohn disease, with less common differential considerations for asymmetrical mural thickening including tuberculous and fungal enterocolitis, as well as malignancy [20]. The spatial resolution of US can nicely illustrate the transmural nature of the disease. Superficial ulceration interrupts the normally

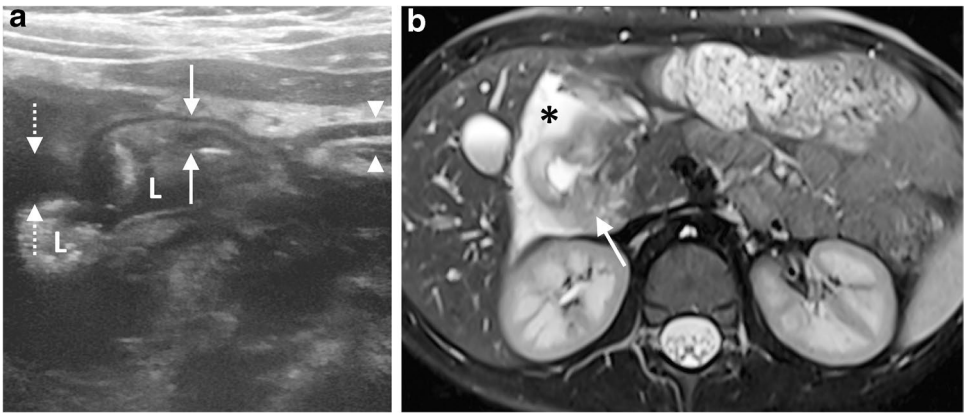

Fig. 2 Spectrum of bowel wall changes in a 5-year-old boy with abdominal pain and large duodenal ulcer on endoscopy. **a** Transverse gray-scale US image of the upper abdomen demonstrates normal mural architecture in the distal stomach (note the superficial antral wall, where the antral lumen is collapsed; *arrowheads*). In the duodenal bulb the superficial wall is progressively thickened but there is preservation of normal stratification (*solid arrows*), while in the second portion of the duodenum there is more severe wall thickening with complete loss of stratification and markedly decreased echogenicity (*dashed arrows*). *L* duodenal lumen. **b** Axial fat-suppressed T2-W image from subsequent MRI confirms the second portion of the duodenum as the region of maximal inflammation, where there is circumferential mural edema and focal irregularity (*arrow*), as well as surrounding free fluid (*asterisk*)

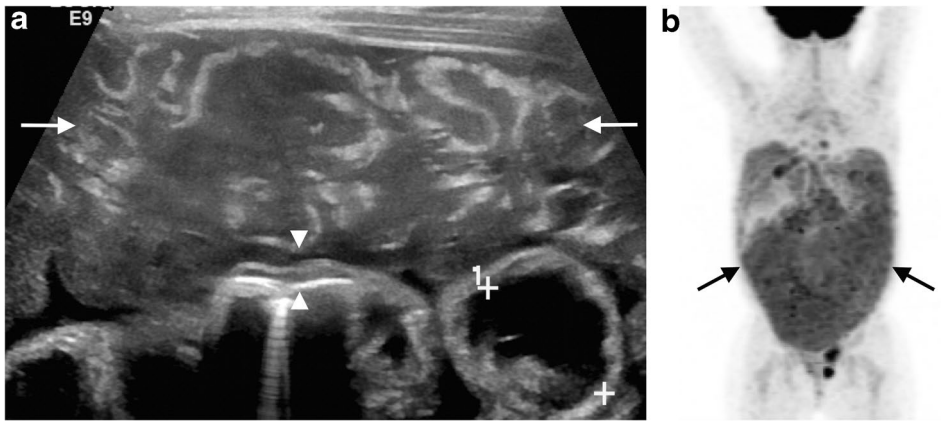

Fig. 3 Disseminated peritoneal rhabdomyosarcoma, which was initially mistaken for abnormal bowel at an outside institution, in a 3-year-old girl. **a** Transverse gray-scale US image of the ventral mid-abdomen demonstrates unusual mixed-echogenicity soft tissue with a cerebriform appearance (*arrows*), vaguely resembling matted bowel loops but lacking the expected multilaminar mural architecture characteristic of subjacent normal bowel (*arrowheads*; calipers placed by the sonographer measure the approximate luminal diameter of an adjacent bowel loop). **b** Subsequent positron emission tomography (PET)/CT shows extensive [F-18]2-fluoro-2-deoxyglucose (FDG)-avidity throughout the entire peritoneal cavity (*arrows*) in the setting of biopsy-proven peritoneal rhabdomyosarcoma

smooth echogenic mucosal interface, producing a cobblestone appearance (Fig. 4), while deeper involvement can result in linear hypoechoic intramural ulcers, serosal penetration with fistula or abscess formation, and stricture [6]. Loss of normal mural stratification is evident with prolonged or severe inflammation and has been correlated with deep ulceration and fissures on histopathology, as well as with need for surgical resection in some series [1, 21]. Such severely affected segments demonstrate fairly homogeneous hypoechogenicity across the mucosa, submucosa and muscularis propria (Fig. 5). In practice, mixed echo patterns often reflect the coexistence of inflammation and fibrosis within diseased bowel segments.

Ulcerative colitis

In contrast to Crohn disease, ulcerative colitis demonstrates a superficial pattern of inflammation characterized by crypt microabscesses and ulceration, usually limited to the mucosa and, in severe cases, the submucosa. The superficial nature of the disease is reflected in its sonographic appearance, marked by mucosal and submucosal thickening with loss of normal haustration (Fig. 6) [22]. Because the process is not transmural, the affected bowel wall shows preserved mural stratification. In distinction to Crohn disease, bowel wall thickening is usually symmetrically circumferential and continuous rather than asymmetrical and discontinuous, and only occasionally affects the terminal ileum on the basis of backwash. Exclusive right colonic involvement is rare, as are abscess and fistula formation [3].

Pseudomembranous colitis

Pseudomembranous colitis is an inflammatory mucosal disease usually caused by an overgrowth of toxin-producing *Clostridium difficile* in the setting of antibiotic treatment. These children present with profuse watery or bloody diarrhea as well as abdominal pain, fever and leukocytosis. On US, there is marked thickening of the colonic wall and together with Crohn disease, pseudomembranous colitis tends to cause the most severe wall thickening among non-neoplastic entities [23]. The thickened bowel wall often demonstrates a heterogeneous intermediate-echogenicity band representing the grossly edematous submucosa and mucosa, with preservation of the normal hypoechoic muscularis propria (Fig. 7) [24]. Mural edema and resultant haustral thickening can efface the lumen of the colon, and linear echogenic structures are occasionally visible parallel to the mucosal interface, reflecting coalescent pseudomembranes [25]. Although there might be relatively little pericolic inflammation given the degree of mural abnormality, ascites is present more commonly than with IBD [23, 24].

Toxic megacolon

Toxic megacolon is an uncommon fulminant transmural colitis that most frequently complicates pseudomembranous and ulcerative colitis. Inflammation and necrosis of smooth muscle in the muscularis propria, along with damage to the myenteric plexus (a component of the enteric nervous system sandwiched between the two layers of muscularis propria

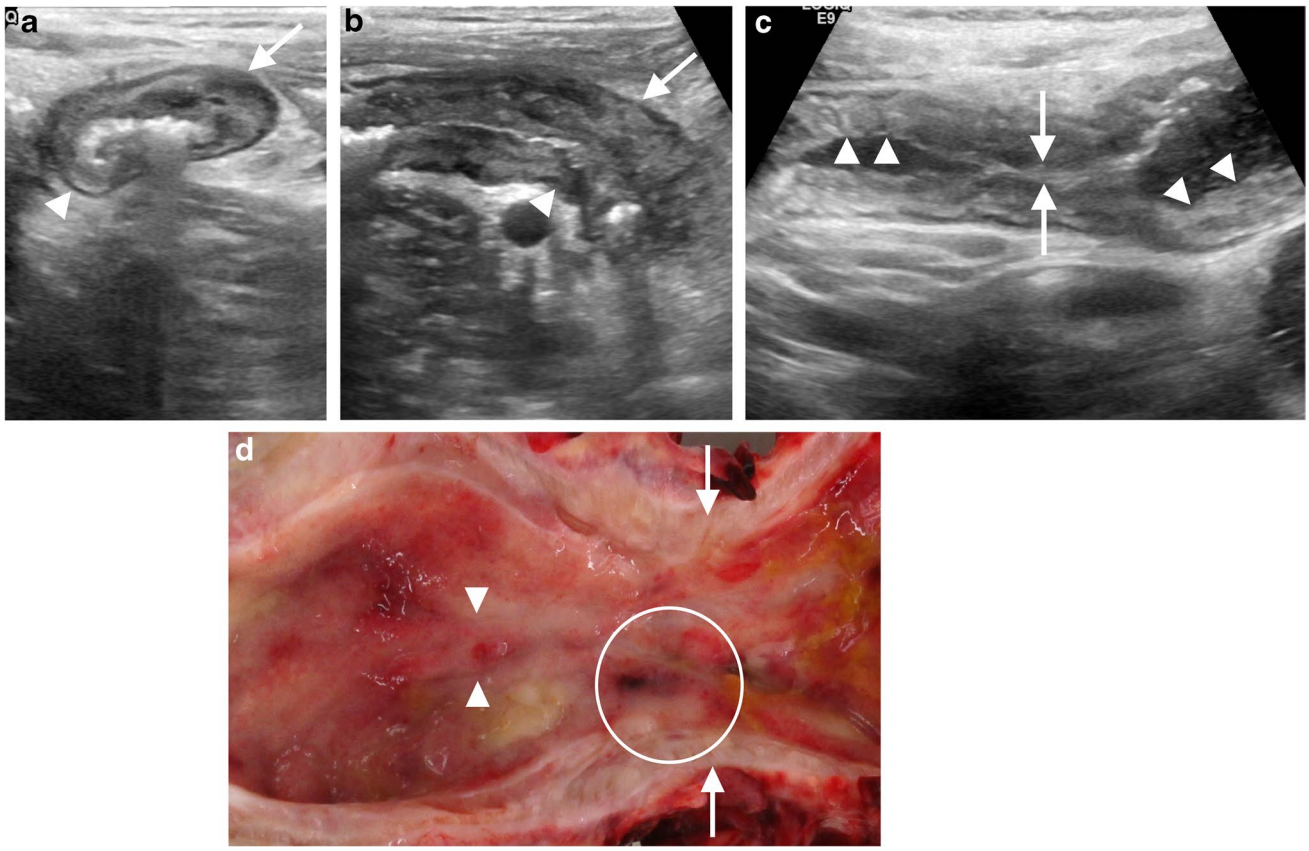

Fig. 4 Penetrating and stricturing Crohn disease manifesting as chronic obstructive symptoms in a 14-year-old boy. He ultimately required ileocecectomy for localized perforation. **a, b** Transverse (**a**) and sagittal (**b**) gray-scale US images of the terminal ileum demonstrate asymmetrical mural thickening, more pronounced along the mesenteric side of the bowel (*arrow*) than the non-mesenteric side (*arrowhead*). **c** Sagittal gray-scale US of the upstream ileum shows irregular contour of the mucosal interface, or cobblestoning (*arrowheads*), reflecting mucosal ulceration, as well as a short segment of luminal narrowing (*arrows*). **d** Gross specimen photo of longitudinally cut small-bowel with the mucosa exposed shows linear ulceration/fissuring (*arrowheads*) and uneven, bumpy mucosal contour (*circle*) reflecting cobblestoning, as well as luminal narrowing (*arrows*)

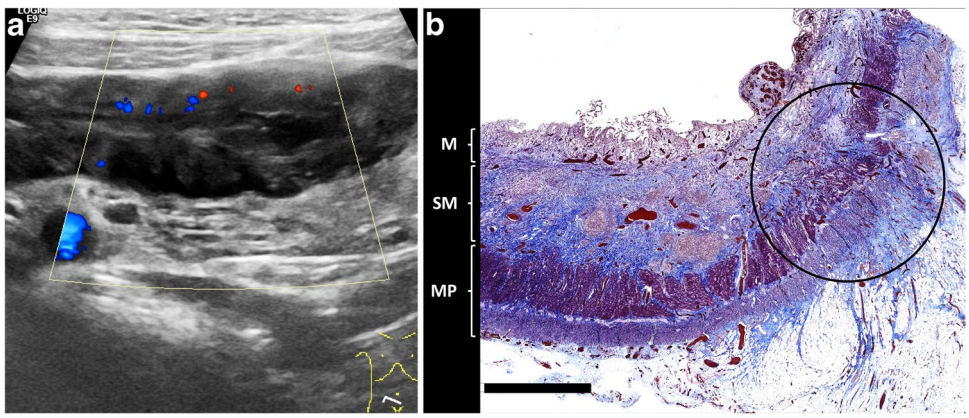

Fig. 5 Stricturing Crohn disease and obstructive symptoms requiring ileocecectomy in a 12-year-old boy. **a** Oblique transverse color Doppler US image of the terminal ileum demonstrates marked mural thickening and loss of normal mural stratification, with heterogeneous hypoechoic appearance of the bowel wall and only minimal hypervascularity. **b** Trichrome stain of resected small bowel (bar=3 mm) shows extensive fibrosis (*blue*) of the submucosa (*SM*) and muscularis propria (*MP*), with marked distortion of the normal multilaminar bowel architecture (*circle*)

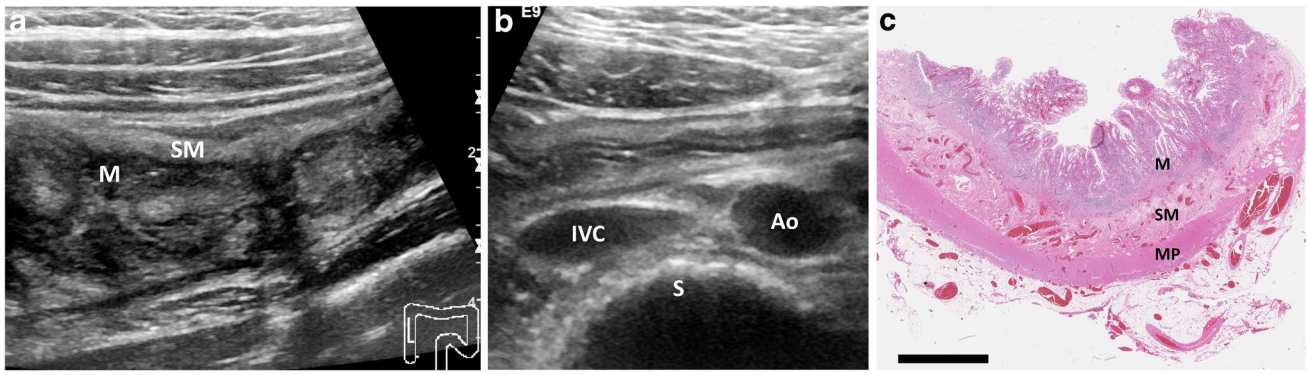

Fig. 6 Ulcerative colitis requiring total colectomy in a 13-year-old boy. **a** Sagittal gray-scale US image of the ascending colon demonstrates mural thickening affecting the hypoechoic mucosa (*M*) to a slightly greater degree than the echogenic submucosa (*SM*). **b** Transverse gray-scale US at the level of the transverse colon shows complete loss of haustration ("lead pipe" appearance). *Ao* aorta, *IVC* inferior vena cava, *S* spine. **c** Hematoxylin and eosin stain from colectomy specimen (bar=4 mm) shows inflammation and thickening disproportionately affecting the mucosa (*M*). The deeper submucosa (*SM*) and muscularis propria (*MP*) show little to no inflammation or fibrosis

smooth muscle), lead to nonobstructive colonic dilation [26]. Colonic dilation and abnormal fold pattern on radiographs along with clinical severity generally dictate management; however, US can be an expeditious portable adjunct in clinically tenuous patients. The diagnosis is suggested on US by the combination of luminal dilation greater than 6 cm (often most marked in the transverse colon) and bowel wall thinning less than 2 mm, with associated loss of haustration (Fig. 8) [27]. Management involves initial treatment of the underlying medical condition. If medical treatment fails, early colectomy prior to colonic perforation should be performed because perforation greatly increases morbidity and mortality [28]. Because subtle free air can be difficult to detect on US, images should be interpreted in conjunction with radiography and with a low threshold for obtaining further cross-sectional imaging.

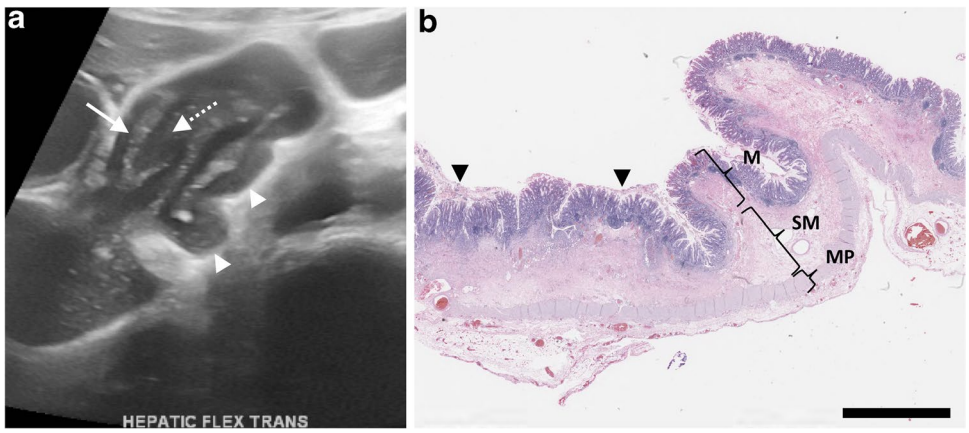

Fig. 7 Pseudomembranous colitis. **a** Transverse gray-scale US image of the hepatic flexure in a 4-year-old girl with Diamond–Blackfan anemia and *C. difficile* colitis demonstrates marked mural thickening with heterogeneous appearance of the echogenic submucosa (*solid arrow*), apparent redundancy of the hypoechoic mucosa from ulceration and sloughing (*dashed arrow*) and thickening of the haustral folds (*arrowheads*). **b** Hematoxylin and eosin stain from colectomy specimen (bar=4 mm) in a different girl, age 16 years, with pseudomembranous colitis shows marked mural and haustral thickening predominantly affecting the mucosa (*M*) and submucosa (*SM*), with relative preservation of normal mural architecture and sparing of the muscularis propria (*MP*). Plaque-like pseudomembranes composed of sloughed necrotic epithelium and inflammatory debris are visible (*arrowheads*)

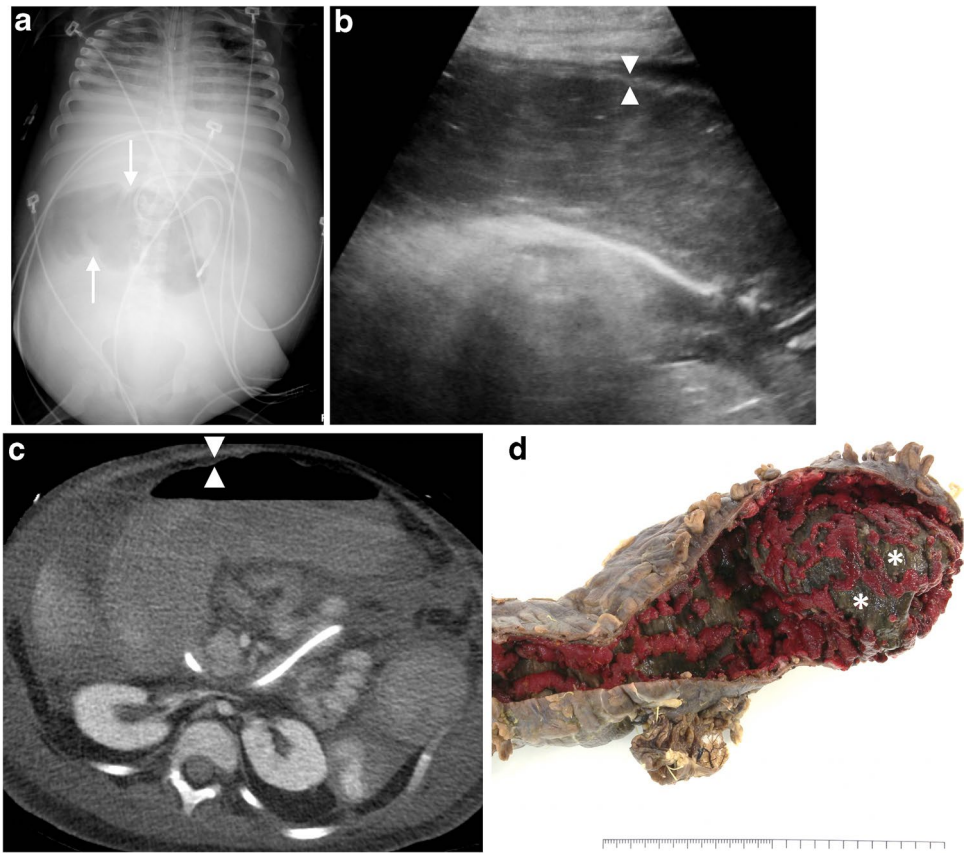

Fig. 8 Toxic megacolon. **a** Abdominal radiograph in a 6-year-old girl with *C. difficile* colitis complicated by toxic megacolon and abdominal compartment syndrome shows a nonspecific abnormal gas pattern with dilation of the transverse colon and haustral blunting (*arrows*). **b** Sagittal gray-scale US of the descending colon in the same girl demonstrates luminal dilation and complete loss of haustration, as well as diffuse thinning (<2 mm) of the bowel wall with loss of the normal laminar architecture (*arrowheads*), a late finding. **c** Immediately subsequent axial contrast-enhanced CT image shows pan-colonic involvement with mural thinning and diminished enhancement, indicating ischemia (*arrowheads*). The girl required total colectomy. **d** Gross specimen photo from a different child, an 11-year-old boy, with toxic megacolon complicating ulcerative colitis shows a dilated colon with a denuded and thinned wall characterized by loss of mucosa and submucosa down to the muscularis propria (*brown*, *asterisks*) and patchy areas of residual mucosa (*red*)

Hemolytic uremic syndrome

Hemolytic uremic syndrome is a thrombotic microangiopathy in which arteriolar or capillary vessel wall damage leads to microvascular thrombosis. More than 90% of cases in children are caused by Shiga toxin–producing *Escherichia coli* infection, with other causes including complement gene mutations, human immunodeficiency virus (HIV) infection and drug toxicity [29, 30]. Pediatric hemolytic uremic syndrome is characterized by the triad of microangiopathic hemolytic anemia, thrombocytopenia and acute kidney injury, and it manifests in the bowel as an acute ischemic pancolitis caused by fibrin thrombi in the submucosal vessels [31].

On US, the colitis appears as concentric mural thickening and partial loss of stratification, with notable avascularity in the acute prodromal stage caused by the thrombotic nature of the disease (Fig. 9). This is followed by bowel reperfusion and hypervascularity, by which time the renal

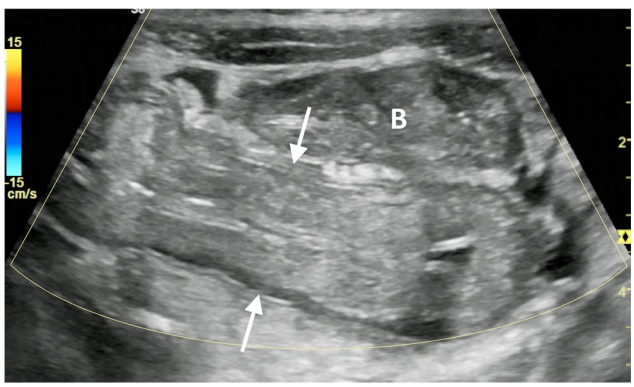

Fig. 9 Hemolytic uremic syndrome in a 3-year-old boy presenting with bloody diarrhea, thrombocytopenia and renal failure after eating an undercooked hamburger. Transverse color Doppler US image of the rectosigmoid colon demonstrates marked circumferential mural thickening and partial loss of stratification without associated hypervascularity (*arrows*) during the initial avascular phase of the disease. Note the bladder (*B*), which is collapsed in the setting of oliguria

and hematological features of the illness are apparent [32]. Recognition of the early avascular phase on US is especially important because colitis often precedes extra-intestinal manifestations, and initial clinical presentation might overlap with intussusception and other infectious and inflammatory diseases.

Other immune-mediated conditions

A variety of immune-mediated conditions can affect the bowel throughout childhood and they range in presentation from malabsorption to acute systemic inflammation. Specific sonographic features are uncommon, so integration of imaging with clinical information and active communication with care team members are critical to contextualize findings. Cow milk protein allergy is a common food allergy in infants and young children, whereby early exposure to cow milk causes immunoglobulin E (IgE)- or non-IgE-mediated polysensitization to its proteins [33]. These children might present with emesis, irritability or bloody diarrhea, and US is occasionally requested to assess for pyloric stenosis or intussusception. Sonographic findings include diffuse bowel wall thickening and hypervascularity, and less commonly pneumatosis intestinalis [34, 35]. Because of potential clinical and radiologic overlap with necrotizing enterocolitis, an awareness of patient history is critical to recognize the benignity of the condition and avoid unnecessary intervention.

Kawasaki disease is a systemic vasculitis affecting medium-size vessels in infancy and early childhood. Nonspecific gastrointestinal complaints are present in one-third of these children in the prodromal or acute phase of disease and might prompt imaging [36]. Bowel US findings are sparsely reported but include segmental non-stratified mural thickening in the small bowel, presumably on the basis of mesenteric vasculitis. Local autonomic dysfunction can also result in focal luminal dilation and pseudo-obstruction [37]. More recently, a Kawasaki-like inflammatory syndrome has been observed in children following infection by severe acute respiratory syndrome coronavirus 2 (SARS-CoV-2), the causal agent of coronavirus disease 2019 (COVID-19). This entity has been designated multisystem inflammatory syndrome in children (MIS-C) [38]. Among its abdominal manifestations, bowel wall thickening in the terminal ileum or right lower quadrant has been reported in 23–57% of cases, probably reflecting the abundance of mucosal lymphoid tissue in this region [39, 40].

Later in childhood, abdominal pain can precede arthralgias or skin rash in immunoglobulin A (IgA) vasculitis and US therefore plays an important role because the radiologist might be the first to suggest the diagnosis. Immune complex deposition in the bowel wall leads to submucosal hemorrhage, producing a stippled or interrupted appearance of the submucosa on US, with loss of stratification portending a more severe disease course [41]. Duodenal and proximal small bowel involvement is common, which might help differentiate IgA vasculitis from other inflammatory conditions. Entero-enteric intussusceptions with intramural hematomas serving as lead points are also frequently encountered and can provide further corroborative evidence of the diagnosis [3, 4].

Vascular anomalies

Vascular anomalies of the gastrointestinal tract are uncommon in children and present with bleeding complications, malabsorption, abdominal pain or intussusception, depending on their location, extent and category within the International Society for the Study of Vascular Anomalies (ISSVA) classification. A variety of syndromic associations mandate appropriate contextual assessment.

Hemangiomas

As in other organ systems, hemangiomas are the most common vascular neoplasm in the pediatric bowel, most frequently affecting the small bowel, and are subdivided into *GLUT1*-positive infantile and *GLUT1*-negative congenital subtypes. Lesions can be focal, multifocal or diffuse and are commonly associated with cutaneous hemangiomas [42]. Focal lesions can appear as intramural, endophytic or exophytic solid vascular masses (Fig. 10), whereas more extensive disease can cause segmental or diffuse bowel wall thickening without a discrete mass. In these latter cases, gray-scale US shows obscuration of normal mural architecture caused by infiltration by anomalous vascular channels. On color Doppler US, marked mural hypervascularity beyond that typically seen with infection or inflammation is suggestive, with spectral Doppler interrogation revealing both arterial and venous waveforms (Fig. 11).

Vascular malformations

Gastrointestinal vascular malformations can be venous, arteriovenous, lymphatic (see next section) or mixed. Arteriovenous malformations are rare outside the setting of hereditary hemorrhagic telangiectasia, while venous malformations occur in isolation or in association with Klippel–Trénaunay, blue rubber bleb nevus and Proteus syndromes, among others [43]. Venous malformations are characterized on US by well-marginated hypoechoic masses or localized thickening of the bowel wall with replacement of the normal stratified mural architecture by hypoechoic lobular venous lakes (Fig. 12). Luminal stenosis is often

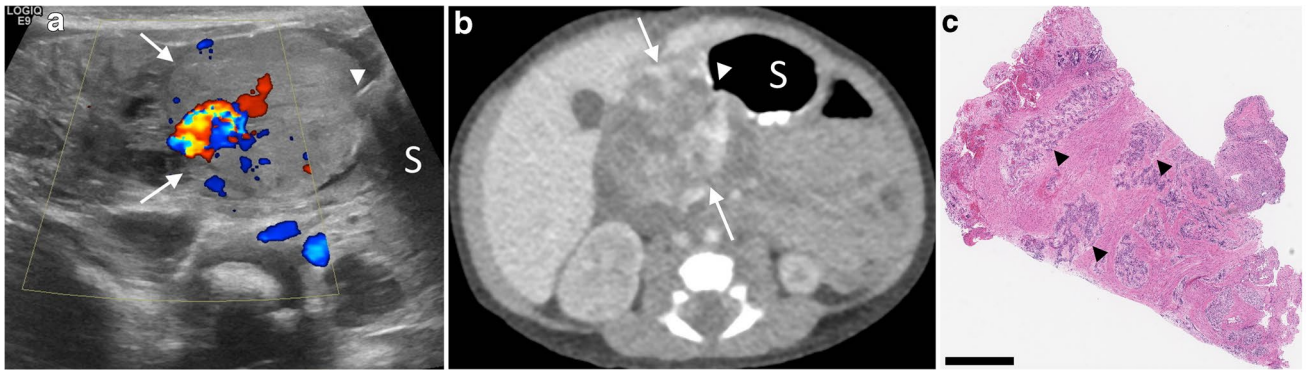

Fig. 10 Gastric outlet obstruction caused by congenital duodenal hemangioma in a 5-day-old girl. **a, b** Transverse color Doppler US (**a**) and axial contrast-enhanced CT (**b**) images demonstrate a predominantly solid vascular mass (*arrows*) in the right upper quadrant directly adjacent to the stomach (*S*), with interrupted peripheral enhancement on CT. Air within the lumen of the gastric outlet is visible coursing into the mass (*arrowhead*), indicating gastrointestinal origin. **c** Hematoxylin and eosin stain of the resected mass (bar=800 μm) shows tufts of capillaries infiltrating the muscularis propria (*arrowheads*). *GLUT1* stain was negative in these capillaries (not shown), excluding infantile hemangioma and confirming congenital hemangioma

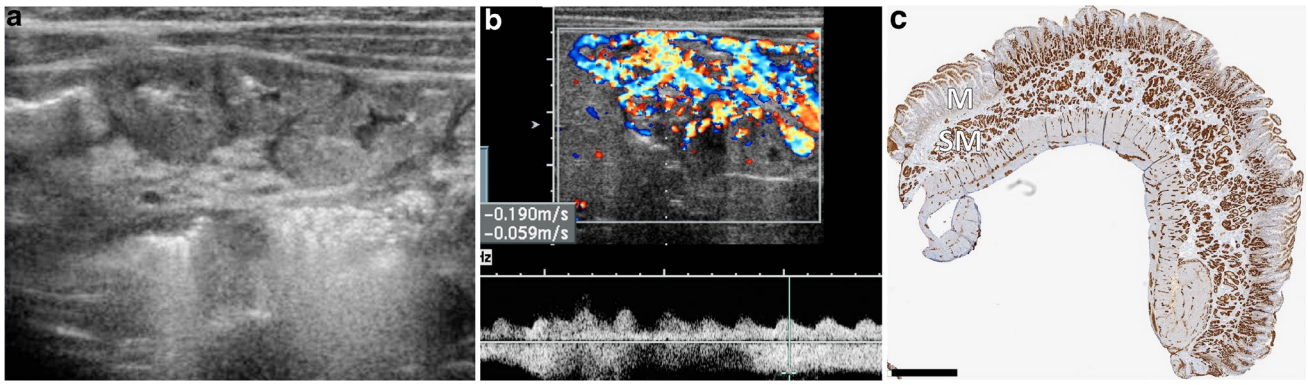

Fig. 11 PHACES syndrome (posterior fossa anomalies, hemangioma, arterial anomalies, cardiac anomalies, eye anomalies and sternal anomalies) and diffuse small bowel hemangiomatosis in a 1-month-old girl presenting with anemia and bloody stools. **a, b** Transverse gray-scale (**a**) and spectral Doppler (**b**) US images of the midabdomen demonstrate mural thickening and obscuration of normal stratification with striking hypervascularity. Both a low-resistance arterial waveform above the baseline and monophasic venous waveform below the baseline are present within the sample volume on spectral Doppler imaging. **c** Cross-section of resected small bowel shows groups of vascular channels throughout the mucosa (*M*) and submucosa (*SM*). Lesional vessels are highlighted by immunohistochemistry for *GLUT1*, characteristic of infantile hemangioma (bar=900 μm)

absent because of the compressible, non-proliferative nature of the lesions [44]. Shadowing phleboliths from intralesional thrombosis and calcification are not always present but are highly characteristic [43]. Color Doppler imaging generally shows a lesser degree of vascularity than seen with hemangiomas.

Primary intestinal lymphangiectasia

Simple lymphatic malformations more commonly affect the mesentery than the bowel; however, primary bowel involvement can be a feature of complex lymphatic disorders. Channel-type lymphatic malformations are disorders of the central conducting lymphatics and can manifest as primary intestinal lymphangiectasia, either in isolation or in conjunction with pulmonary lymphangiectasia. Dysplastic, non-proliferating lymphatics in the bowel impair normal drainage and produce a protein-losing enteropathy with diarrhea, peripheral edema and lymphocytopenia [45]. Intestinal lymphangiectasia occurs sporadically or in association with Down, Turner or Noonan syndromes [46].

The sonographic findings of intestinal lymphangiectasia include diffuse or segmental bowel wall thickening and mesenteric edema, as well as ascites and generalized thickening of hollow viscera [47]. Mural hypervascularity is notably absent, which differentiates intestinal lymphangiectasia from

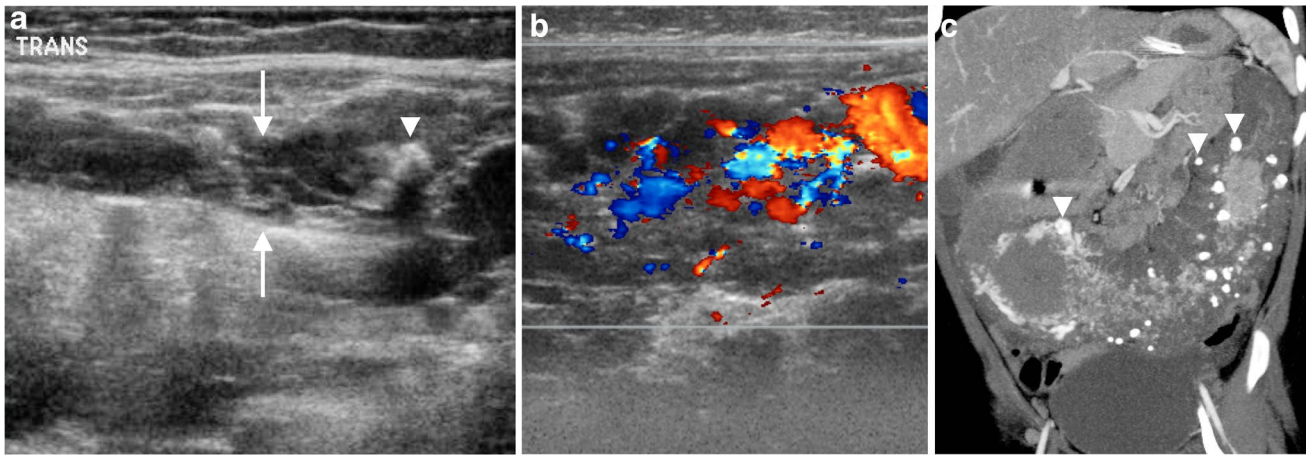

Fig. 12 Recurrent intussusceptions and diffuse colonic venous malformation in a 1-year-old girl. **a, b** Transverse gray-scale (**a**) and color Doppler (**b**) US images of the transverse colon demonstrate mural thickening and replacement of the normal mural architecture by numerous lobular hypoechoic spaces (*arrows*), irregular shadowing intramural calcification (*arrowhead*) and disorganized hypervascularity. **c** Coronal maximum-intensity projection from subsequent contrast-enhanced CT shows the extent of diffuse mural thickening, with patchy enhancement and multiple intramural phleboliths (*arrowheads*)

many other entities causing bowel wall thickening (Fig. 13). In the authors' experience, the dilated central conducting lymphatics seen on conventional or MR lymphangiography are not reliably visualized on US.

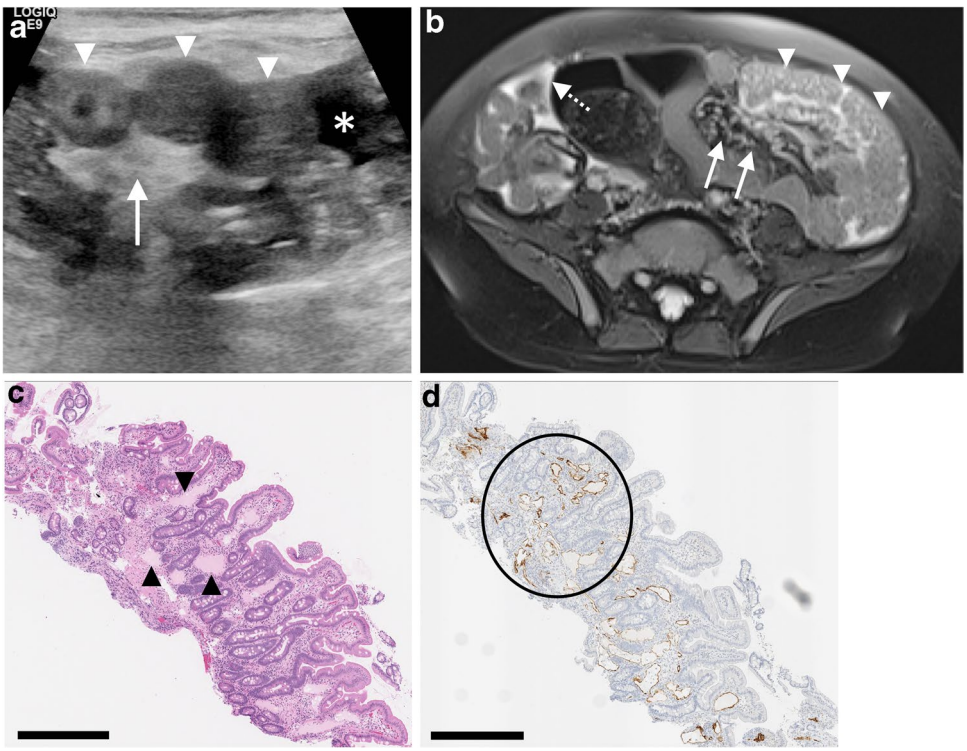

Fig. 13 Noonan syndrome and diffuse lymphangiectasia (pulmonary and intestinal) in a 3-year-old boy. **a** Transverse gray-scale US image of the lower abdomen shows nonspecific mural thickening of small bowel loops (*arrowheads*) with adjacent mesenteric edema (*arrow*) and simple free fluid (*asterisk*). **b** Axial fat-suppressed T2-W MR image reveals nodular small bowel thickening with obscuration of the normal fold pattern and suggestion of tiny stippled cystic spaces (*arrowheads*). Engorgement of the associated mesentery (*solid arrows*) is on the basis of dilated lymphatics rather than hypervascularity and there is chylous ascites (*dashed arrow*). **c, d** Hematoxylin and eosin stain from small-bowel mucosal biopsy (**c**) shows dilated lymphatic channels in the lamina propria (*arrowheads*), positive by immunohistochemistry (**d**) for the lymphatic marker D2–40 (*circle* in **d**). Bars=500 µm

Neoplasm

Lymphoma

Lymphoma is the most common malignancy of the small bowel in children, arising both primarily and secondarily in the setting of post-transplant lymphoproliferative disorder. The terminal ileum is frequently involved and colonic involvement is rare. Intestinal lymphoma is usually of the Burkitt type of non-Hodgkin disease, and might present with a rapidly growing abdominal mass or with nonspecific abdominal pain and emesis. Burkitt lymphoma appears on US as a hypoechoic circumferential or mural-based solitary mass, and bowel wall thickening is often massive and out of proportion to that seen with most other etiologies (Fig. 14). Mural architecture is lost because of a combination of lymphatic obstruction and tumor infiltration, with destruction of the muscularis propria and obliteration of the autonomic nerve plexus resulting in aneurysmal dilatation of the bowel lumen [8, 48, 49]. Complete obstruction is uncommon, even with marked mural thickening, because the tumor tends not to incite a desmoplastic response [8].

Other masses

A variety of other neoplasms occur infrequently in the pediatric gastrointestinal tract, including gastrointestinal stromal tumor, adenocarcinoma, leiomyosarcoma and carcinoid tumor. Gastrointestinal stromal tumor arises from the interstitial cells of Cajal in the muscularis propria and might appear as exophytic, intramural or endophytic masses of variable echogenicity. Larger exophytic lesions often demonstrate cystic changes and tend to be less vascular than smaller submucosal tumors [50]. Associated conditions include neurofibromatosis type 1 and Carney triad, and involvement distal to the stomach is uncommon. Adenocarcinoma is likewise extremely rare in children, and can occur sporadically or in the setting of polyposis syndromes or microsatellite instability. US might demonstrate an exophytic polypoid mass with variable necrosis, focal eccentric wall thickening, or more diffuse circumferential wall thickening mimicking inflammatory processes or lymphoma (Fig. 15) [51, 52].

Conclusion

Ultrasound is an excellent tool for assessing bowel pathology and offers a distinct opportunity to evaluate the bowel wall in a more granular fashion. An understanding of normal and abnormal bowel wall architecture can facilitate the provision of more nuanced interpretation and expansion of differential considerations.

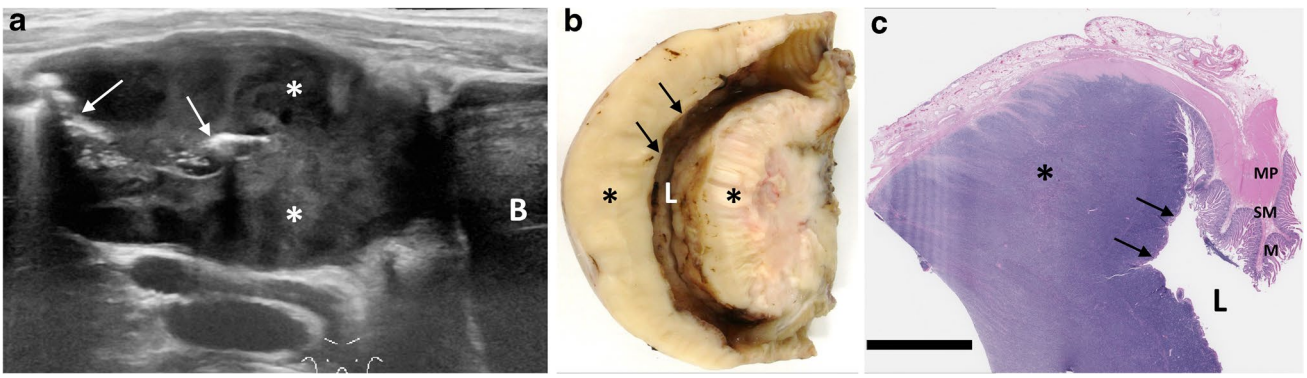

Fig. 14 Burkitt lymphoma in an 8-year-old boy presenting with acute abdominal pain. **a** Sagittal gray-scale US image of the lower abdomen demonstrates massive mural thickening of the ileal wall with complete loss of mural stratification (*asterisks*). The bowel lumen can be seen traversing the mass (*arrows*). *B* bladder. **b** Gross specimen photo of the longitudinally sectioned ileum following diagnostic laparoscopy and segmental ileal resection shows the tumor circumferentially invading the bowel wall (*asterisks*). The overlying mucosa is intact but effaced (*arrows*) and the plicae are not evident. A segment of uninvolved ileum with normal mucosal folds can be seen at top right. *L* bowel lumen. **c** Hematoxylin and eosin stain from representative section (bar=4 mm) shows tumor invading and expanding the submucosa and muscularis propria (*asterisk*), with effacement of the mucosa (*arrows*). The normal mucosa (*M*), submucosa (*SM*) and muscularis propria (*MP*) are seen at the right of the image

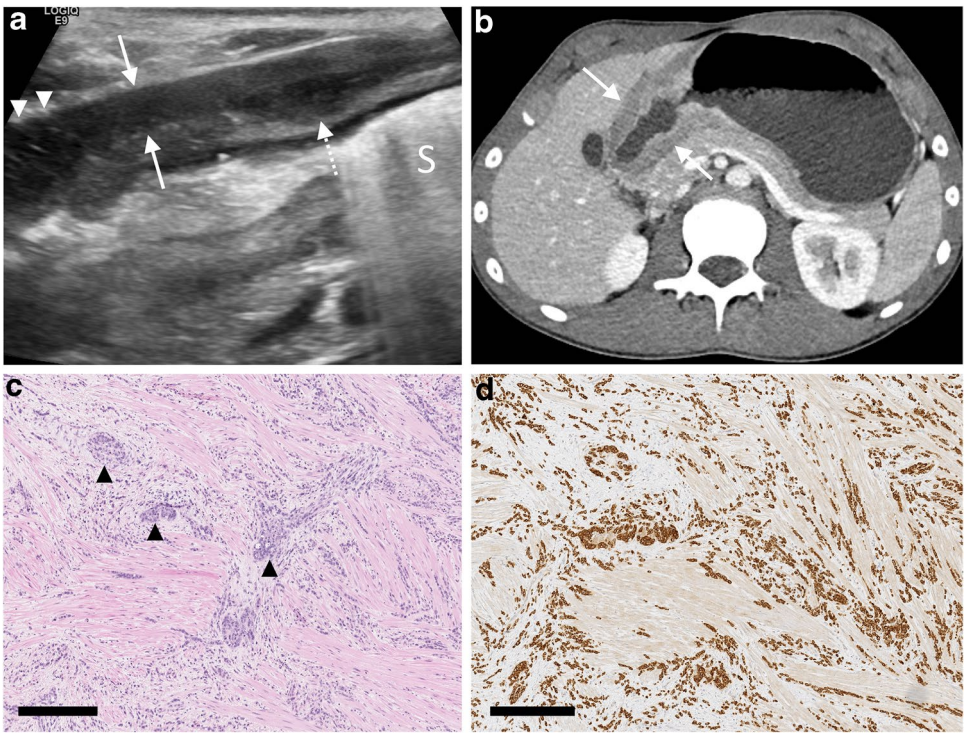

Fig. 15 Biopsy-proven diffuse infiltrative gastric carcinoma in a 14-year-old boy with progressive gastric outlet obstruction. The boy had undergone bone marrow transplant as an infant for hemophagocytic lymphohistiocytosis but had no other cancer predisposition. **a** Transverse gray-scale US image of the pylorus demonstrates diffuse mural thickening, most pronounced involving the muscularis propria (*solid arrows*). Mural stratification is relatively preserved, although the interfaces between the muscularis propria and both the submucosa (*dashed arrow*) and the serosa (*arrowheads*) appear irregular. *S* denotes air within the gastric lumen. **b** Axial contrast-enhanced CT image shows irregular pyloric wall thickening (*solid arrows*) without delineation of mural architecture. **c, d** Hematoxylin and eosin stain from antral wall biopsy (**c**) shows infiltrating nests and cords of malignant cells throughout the muscularis propria (*arrowheads*), positive by immunohistochemistry (**d**) for the epithelial marker AE1/AE3 (pan-keratin). Bars=300 μm

Declarations

Conflicts of interest None

References

1. Alison M, Kheniche A, Azoulay R et al (2007) Ultrasonography of Crohn disease in children. Pediatr Radiol 37:1071–1082
2. Darge K, Anupindi S, Keener H et al (2010) Ultrasound of the bowel in children: how we do it. Pediatr Radiol 40:528–536
3. Anupindi SA, Halverson M, Khwaja A et al (2014) Common and uncommon applications of bowel ultrasound with pathologic correlation in children. AJR Am J Roentgenol 202:946–959
4. Francavilla ML, Anupindi SA, Kaplan SL et al (2017) Ultrasound assessment of the bowel: inflammatory bowel disease and conditions beyond. Pediatr Radiol 47:1082–1090
5. Atkinson NSS, Bryant RV, Dong Y et al (2017) How to perform gastrointestinal ultrasound: anatomy and normal findings. World J Gastroenterol 23:6931–6941
6. Elliott CL, Maclachlan J, Beal I (2018) Paediatric bowel ultrasound in inflammatory bowel disease. Eur J Radiol 108:21–27
7. Rao JN, Wang JY (2010) Regulation of gastrointestinal mucosal growth. Morgan & Claypool Life Sciences, San Rafael
8. Muradali D, Goldberg DR (2015) US of gastrointestinal tract disease. Radiographics 35:50–68
9. Gale HI, Gee MS, Westra SJ et al (2016) Abdominal ultrasonography of the pediatric gastrointestinal tract. World J Radiol 8:656–667
10. Chiorean L, Schreiber-Dietrich D, Braden B et al (2014) Transabdominal ultrasound for standardized measurement of bowel wall thickness in normal children and those with Crohn's disease. Med Ultrason 16:319–324
11. Haber HP, Stern M (2000) Intestinal ultrasonography in children and young adults: bowel wall thickness is age dependent. J Ultrasound Med 19:315–321
12. Fortman BJ, Kuszyk BS, Urban BA et al (2001) Neurofibromatosis type 1: a diagnostic mimicker at CT. Radiographics 12:601–612
13. Levy AD, Patel N, Dow N et al (2005) From the archives of the AFIP: abdominal neoplasms in patients with neurofibromatosis type 1: radiologic–pathologic correlation. Radiographics 25:455–480
14. Dillman JR, Smith EA, Morani AC, Trout AT (2017) Imaging of the pediatric peritoneum, mesentery and omentum. Pediatr Radiol 47:987–1000

15. Leung RS, Calder A, Roebuck D (2009) Embryonal rhabdomyosarcoma of the omentum: two cases occurring in children. Pediatr Radiol 39:865–868
16. Maaser C, Sturm A, Vavrick SR et al (2019) ECCO-ESGAR guidelines for diagnostic assessment in IBD part 1: initial diagnosis, monitoring of known IBD, detection of complications. J Crohns Colitis 13:144–164
17. Gokli A, Dillman JR, Humphries PD et al (2021) Contrast-enhanced ultrasound of the pediatric bowel. Pediatr Radiol 51:2214–2228
18. Lu C, Merrill C, Medellin A (2019) Bowel ultrasound state of the art: grayscale and Doppler ultrasound, contrast enhancement, and elastography in Crohn disease. J Ultrasound Med 38:271–288
19. Biko DM, Rosenbaum DG, Anupindi SA (2015) Ultrasound features of pediatric Crohn disease: a guide for case interpretation. Pediatr Radiol 45:1557–1566
20. Bruining DH, Zimmerman EM, Loftus EV Jr et al (2018) Consensus recommendations for evaluation, interpretation, and utilization of computed tomography and magnetic resonance enterography in patients with small bowel Crohn's disease. Radiology 286:776–799
21. Rosenbaum DG, Conrad MA, Biko DM et al (2017) Ultrasound and MRI predictors of surgical bowel resection in pediatric Crohn disease. Pediatr Radiol 47:55–64
22. Maconi G, Radice E, Greco S, Porro GB (2006) Bowel ultrasound in Crohn's disease. Best Pract Res Clin Gastroenterol 20:93–112
23. d'Almeida M, Jose J, Oneto J, Restrepo R (2008) Bowel wall thickening in children: CT findings. Radiographics 28:727–746
24. Downey DB, Wilson SR (1991) Pseudomembranous colitis: sonographic features. Radiology 180:61–64
25. Ramachandran I, Sinha R, Rodgers P (2006) Pseudomembranous colitis revisited: spectrum of imaging findings. Clin Radiol 61:535–544
26. Sheth SG, LaMont JT (1998) Toxic megacolon. Lancet 351:509–513
27. Maconi G, Sampietro GM, Ardizzone S et al (2004) Ultrasonographic detection of toxic megacolon in inflammatory bowel diseases. Dig Dis Sci 49:138–142
28. Ausch C, Madoff RD, Gnant M et al (2006) Aetiology and surgical management of toxic megacolon. Color Dis 8:195–201
29. Ardissino G, Salardi S, Colombo E et al (2016) Epidemiology of haemolytic uremic syndrome in children. Data from the North Italian HUS Network. Eur J Pediatr 175:465–473
30. Loirat C, Fakhouri F, Ariceta G et al (2016) An international consensus approach to the management of atypical hemolytic uremic syndrome in children. Pediatr Nephrol 31:15–39
31. Kawanami T, Bowen AD, Girdany BR (1984) Enterocolitis: prodrome of the hemolytic-uremic syndrome. Radiology 151:91–92
32. Baud C, Saguintaah M, Veyrac C et al (2004) Sonographic diagnosis of colitis in children. Eur Radiol 14:2105–2119
33. Wal JM (2004) Bovine milk allergenicity. Ann Allergy Asthma Immunol 95:S2–S11
34. Epifanio M, Spolidoro JV, Soder RB et al (2011) Gray-scale and color Doppler ultrasound findings in children with cow's milk allergy. AJR Am J Roentgenol 196:W817–W822
35. Siddique Z, Thibodeau R, Jafroodifar A et al (2021) Pediatric milk protein allergy causing hepatic portal venous gas: case report. Radiol Case Rep 16:246–249
36. Yaniv L, Jaffe M, Shaoul R (2005) The surgical manifestations of the intestinal tract in Kawasaki disease. J Pediatr Surg 40:e1–e4
37. Maurer K, Unsinn KM, Waltner-Romen M et al (2008) Segmental bowel-wall thickening on abdominal ultrasonography: an additional diagnostic sign in Kawasaki disease. Pediatr Radiol 38:1013–1016
38. Centers for Disease Control and Prevention (2020) Multisystem inflammatory syndrome in children (MIS-C) associated with coronavirus disease 2019 (COVID-19). CDC website. https://emergency.cdc.gov/han/2020/han00432.asp. Accessed 28 May 2021
39. Fenlon EP III, Chen S, Ruzal-Shapiro CB et al (2021) Extracardiac imaging findings in COVID-19-associated multisystem inflammatory syndrome in children. Pediatr Radiol 51:831–839
40. Caro-Dominguez P, Navallas M, Riaza-Martin L et al (2021) Imaging findings of multisystem inflammatory syndrome in children associated with COVID-19. Pediatr Radiol 51:1608–1620
41. Nchimi I, Khamis J, Paquot I et al (2008) Significance of bowel wall abnormalities at ultrasound in Henoch-Schonlein purpura. J Pediatr Gastroenterol Nutr 46:48–53
42. Fishman SJ, Mulliken JB (1993) Hemangiomas and vascular malformations of infancy and childhood. Pediatr Clin N Am 40:1177–1200
43. Dubois J, Rypens F, Garel L et al (2007) Pediatric gastrointestinal vascular anomalies: imaging and therapeutic issues. Pediatr Radiol 37:566–574
44. Zhang M, Lin H, Qin LL (2021) Sonography of pediatric gastrointestinal venous malformations. J Clin Ultrasound 49:269–273
45. Trenor CC 3rd, Chaudry G (2014) Complex lymphatic anomalies. Semin Pediatr Surg 23:186–190
46. Malone LJ, Fenton LZ, Weinman JP et al (2015) Pediatric lymphangiectasia: an imaging spectrum. Pediatr Radiol 45:562–569
47. Dorne HL, Jequier S (1986) Sonography of intestinal lymphangiectasia. J Ultrasound Med 5:13–16
48. Kaste SC, McCarville MB (2008) Imaging pediatric abdominal tumors. Semin Roentgenol 43:50–59
49. Miller JH, Hindman BW, Lam AH (1980) Ultrasound in the evaluation of small bowel lymphoma in children. Radiology 135:409–414
50. Furman MS, Connolly SA, Brown SD, Callahan MJ (2020) The pediatric stomach — masses and mass-like pathology. Pediatr Radiol 50:1180–1190
51. Lin CH, Lin WC, Lai IH et al (2015) Pediatric gastric cancer presenting with massive ascites. World J Gastroenterol 21:3409–3413
52. Hill DA, Furman WL, Billups CA et al (2007) Colorectal carcinoma in childhood and adolescence: a clinicopathologic review. J Clin Oncol 25:5808–5814